Fibers and Polymers 2016, Vol.17, No.11, 1741-1748
DOI 10.1007/s12221-016-6747-6

ISSN 1229-9197 (print version)
ISSN 1875-0052 (electronic version)

Dissolution and Regeneration Behavior of Chitosan in 3-methyl-1-(ethylacetyl)imidazolium Chloride

Bin Xu, Qiaoping Li, Linghua Zhuang[1], Qiang Wang[1], Chao Li[1], Guowei Wang*†, Fengwei Xie[2†], and Peter J. Halley[2]

College of Food Science and Light Industry, Nanjing Tech University, Nanjing 211816, China
[1]*College of Chemistry and Molecular Engineering, Nanjing Tech University, Nanjing 211816, China*
[2]*School of Chemical Engineering, The University of Queensland, Brisbane Qld 4072, Australia*
(Received July 22, 2016; Revised September 28, 2016; Accepted October 2, 2016)

Abstract: 3-methyl-1-(ethylacetyl)imidazolium chloride ([EtMIM]Cl), was synthesized for chitosan dissolution, and the dissolution and regeneration behaviors of chitosan in [EtMIM]Cl were thoroughly investigated. The solubility of chitosan in [EtMIM]Cl was measured at temperatures ranging from 40 °C to 110 °C, based on which the thermodynamic parameters of chitosan in [EtMIM]Cl were calculated. The polarizability and hydrogen bond accepting ability was determined by solvatochromic UV/vis spectroscopy. The regenerated chitosan from [EtMIM]Cl by adding methanol was characterized by thermogravimetric analysis (TGA), Fourier transform infrared spectroscopy (FTIR), X-ray diffraction (XRD) and scanning electron microscopy (SEM). Density functional theory (DFT) computations were performed to study the interactions between [EtMIM]Cl and chitobiose. Five kinds of hydrogen bonds, C-H/O, O-H/O, O-H/Cl, C-H/Cl, N-H/Cl were found, suggesting strong interactions between [EtMIM]Cl and chitobiose. In particular, the oxygen atom and the active methylene group of carboxylic ester in $[EtMIM]^+$, formed strong hydrogen bonding with chitobiose. The molecular simulation results indicated that both the Cl^- anions and $[EtMIM]^+$ cation played important roles in the chitosan dissolution process, by the disruption of native hydrogen bonds of chitosan.

Keywords: Ionic liquids, Chitosan, Dissolution, Regeneration, Molecular simulation

Introduction

Chitosan, the deacetylated form of chitin, is composed of D-glucosamine units joined by β-(1-4) glucosidic bonds (Figure 1) [1-3]. Due to its low toxicity, biocompatibility and antimicrobial activity, chitosan is widely applied in the fields of fertilizers, ion-exchange resins, membrane separation, pharmaceutics, cosmetics etc [4-6]. Despite of its appealing advantages, the application of chitosan is limited due to its poor solubility in normal solvents. Some solvents showed good solubility for chitosan, such as acetic acid, trifluoroacetic acid and hexafluoro-2-propanol [7,8]. But they are generally volatile, toxic or corrosive, which may lead to serious environmental problems. Besides, it is difficult to recover these solvents after dissolution, which may increase the costs in practical applications and cause further environmental problems. Therefore, to enhance and widen chitosan applications, it is highly important to design and synthesize novel solvents for chitosan dissolution.

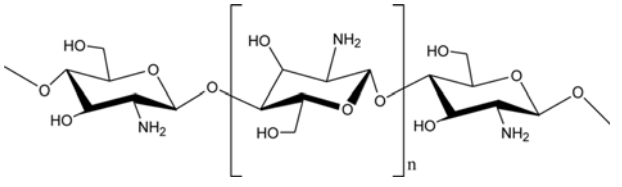

Figure 1. Schematic structure of chitosan.

Ionic liquids (ILs) are defined as organic molten salts with melting temperature below 100 °C. ILs have unique properties, such as non-detectable vapor pressure, low melting point, high chemical and thermal stability, non-flammability, and chemical tunabilities, which make them have been extensively applied in catalytic reactions, organic synthesis, functional materials, life science and electrochemical reactions [9-14]. Research has shown that ILs is effective for the dissolution of cellulose [15-21]. Some ILs have been applied in practical process [22-25], including chloride, formate and acetate as anions, and 1-allyl-3-methylimidazolium ([AMIM]), 1-butyl-3-methylimidazolium ([BMIM]) and 1-ethyl-3-dimethylimidazolim ([EMIM]) as cations. However, there have been limited studies on the dissolution of chitosan using ILs. Past work considered IL anion as the decisive factor in the dissolution of chitosan [26,27], while the effect of cation in ILs is seldom considered. Nevertheless, it is worth to explore the effects of the IL cation on the biopolymer dissolution, and the related dissolution mechanism.

In this work, an ionic liquid, 3-methyl-1-(ethylacetyl) imidazolium chloride ([EtMIM]Cl), containing carboxylic acid ester group in cationic group, was synthesized from ethyl chloroacetate and 1-methylimidazole. Compared to the conventional imidazolium-based ionic liquids ($BMIM^+$, $EMIM^+$), carboxylic acid ester cationic group in [EtMIM]Cl have more electronegative ester groups and stronger electronic cloud density of oxygen atoms, [EtMIM]Cl is easier to destroy the intermolecular or intramolecular

*Corresponding author: kingwell2004@sina.com
†These authors equally contributed to the manuscript.

hydrogen bonds in chitosan, so as to accelerate the dissolution of chitosan in [EtMIM]Cl.

In this work, the solubility of chitosan in [EtMIM]Cl was measured as a function of temperature. Thermodynamic parameters of chitosan in [EtMIM]Cl were calculated from the solubility data. The polarizability and hydrogen bond accepting ability was determined by solvatochromic UV/vis spectra. The regenerated chitosan from [EtMIM]Cl by addition of methanol was characterized by thermogravimetric analysis (TGA), Fourier transform infrared spectroscopy (FTIR), X-ray diffraction (XRD) and scanning electron microscopy (SEM). In addition, density functional theory (DFT) computations were carried out to discuss the interactions between the [EtMIM]Cl and chitosan. The effect of cationic structure (especially the active atoms in carboxylic acid ester) on the solubility of chitosan was discussed.

Experimental

Materials

Chitosan with a deacetylation degree of 90-95 % and viscosity of 60-100 cps was purchased from Jinhu County, Huantai Shell Products Co., Ltd., and was dried at 85 °C in a vacuum oven for 8h to remove the original water content. 1-methylimidazole (99 %), ethyl chloroacetate, 4-nitroaniline (98.0 %) and N,N-Diethyl-4-nitroaniline (97.0 %) were purchased from Sinopharm Chemical Reagent Co., Ltd.. Methanol and other organic or inorganic compounds were purchased from Shanghai Aladdin Industrial Chemical Co., Ltd. [EtMIM]Cl, as shown in Figure 2, was synthesized by ethyl chloroacetate and 1-methylimidazole according to the method previously reported [28]. The [EtMIM]Cl was dried under vacuum at 70 °C for over 24 h, and the water content of [EtMIM]Cl was determined by the Karl Fischer titration (<1000 ppm).

^{1}H NMR Spectroscopy

The chemical structure of [EtMIM]Cl was established by nuclear magnetic resonance spectroscopy (^{1}H-NMR) at room temperature. ^{1}H-NMR spectra were recorded on the AVANCE AV-300 or AVANCE AV-500 (Bruker Co. Ltd., Germany) operating at 500 MHz and chemical shifts were given in ppm units relative to tetramethylsilane (TMS). The splitting patterns are designated as follows: s, singlet; d, doublet; t, triplet; q, quartet; and m, multiplet.

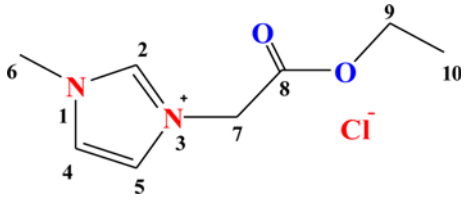

Figure 2. Chemical structure of [EtMIM]Cl.

Determination of Deacetylation Degree and Molecular Weight

Alkaline method was used to measure deacetylation degree (DD) of chitosan. At room temperature, the dried chitosan (0.25 g) was added in 20 m*l* of 0.1 M hydrochloric acid (HCl) by magnetic stirring for 10 h. The impurities were removed by filtration, then a small amount of methyl orange was added as the indicator. After that, 0.1 M aqueous sodium hydroxide (NaOH) was added to adjust the pH of the solution. The volume of NaOH was recorded when the solution turned to yellow. DD of chitosan was calculated by the following equation:

$$(\text{-NH}_2)\% = \frac{(c_1 v_1 - c_2 v_2) \times 0.016}{G} \times 100\% \quad (1)$$

$$\text{DD} = \frac{(\text{-NH}_2)\%}{9.94\%} \times 100\% \quad (2)$$

where c_1 and c_2 stand for the concentrations of HCl and NaOH respectively and v_1 and v_2 represent the volumes of HCl and NaOH respectively, and G is the sample weight.

The molecular weight of chitosan was determined by viscometry with the application of the Mark-Houwink equation [29]. Chitosan was dissolved in 0.2 M sodium chloride-0.1 M acetic acid aqueous solution. The measurements were performed at 25 °C. The molecular weight (M_v) of chitosan was calculated by the following equation:

$$[\eta] = K^{\circ} \overline{Mv^{\alpha}} \quad (3)$$

where η is the intrinsic viscosity, K=1.81×10^{-3} and α=0.93, respectively.

Dissolution of Chitosan in Ionic Liquids

The dried [EtMIM]Cl (about 5.0 g) was added in a sealed colorimetric tube, which was then immersed in an oil bath. The temperature instability of the oil bath was estimated to be ±1 °C. Under continuous magnetic stirring, finely-ground chitosan powder (0.2 wt% of the [EtMIM]Cl) was added. The mixture started from 40 °C. Additional chitosan (another 0.2 wt% of the IL) was added until the solution became clear, and it can be considered that the chitosan became saturated when it could not be dissolved further within 2 h. The temperature was increased with 10 °C intervals, up to a maximum temperature of 110 °C. Then the solubility of the chitosan at the given temperature was determined. According to the amount of [EtMIM]Cl and dissolved chitosan, the thermodynamic parameters of chitosan in [EtMIM]Cl at a given temperature were calculated.

The solubility of chitosan in [BMIM]Cl followed above mentioned procedure.

Measurements of β and π^* Parameters of the [EtMIM]Cl

According to the procedure reported previously [30], β and π^* parameters were determined by the absorption peaks of the dyes, N,N-diethyl-4-nitro-aniline (DENA) and 4-nitroaniline (NA). By adding the dyes in dry methanol, the concentrated solution was prepared. The solution and a given amount of the [EtMIM]Cl were added and mixed homogeneously. The methanol was removed under vacuum at 40 °C for over 12 h, and then [EtMIM]Cl solution was added into a quartz cell in a dry box. The λ_{max} was measured through a carry 60 ultraviolet visible spectrophotometer at 25.0±0.1 °C.

Regeneration of Chitosan

To achieve the regenerated chitosan, methanol was added to the mixture of [EtMIM]Cl-chitosan. [EtMIM]Cl (5 g) and chitosan (2.0 wt%) solution were prepared in the regeneration trial. Methanol (20 m*l*) were added to the [EtMIM]Cl-chitosan solution, and stirred for 30 min at room temperature. The precipitated chitosan was washed four times to ensure complete chitosan regeneration. After vaporizing the residual methanol, the regenerated chitosan was dried under vacuum at 60 °C for 12 h.

Characterization of Chitosans

FT-IR spectra of different chitosan samples were recorded using a Nicolet 5700 FT-IR spectrometer (Thermo Electron Corporation, Madison, WI, USA) equipped with a Nicolet Smart Orbit attenuated total reflectance (ATR) accessory incorporating a diamond internal reflection element. For each spectrum, 64 scans were recorded over the range of 4000-500 cm^{-1} at 22 °C at a resolution of 4 cm^{-1}. The background spectrum was recorded on air and subtracted from the sample spectrum.

Mettler Toledo TGA machine (Mettler-Toledo Ltd., Port Melbourne, Australia) was used with 40 μl aluminium crucibles for thermogravimetric analysis (TGA) under nitrogen. A sample mass of about 5 mg was used for each run. The samples were heated from 40 °C to 500 °C and measured in the dynamic heating regime, using a constant heating ramp of 10 K/min.

XRD patterns were collected on a SmartLab-3kw XRD diffractometer with Cu-Kα radiation (λ=0.154 nm) over the range 5-60 degrees (2θ) at a scan speed of 2 degrees (2θ) per minute.

SEM photomicrographs were recorded on TM3000 scanning electron microscope (HITACHI, Japan) at an accelerating voltage of 20 kV. The free surfaces of the regenerated chitosan were coated with thin layers of gold before observation.

Computational Methods

In order to simplify the calculations, chitobiose was chosen as the representative structure of the chitosan, as shown in Figure 9 [31]. The geometries of chitobiose, [EtMIM]Cl, and the complex of the [EtMIM]Cl and chitobiose were fully optimized at B3LYP/6-31G(d,p) [32] level. All calculations were carried out using Gaussian 09 program package (revision B.01; Gaussian, Inc., Wallingford CT, 2010) [33].

Results and Discussion

^{1}H NMR of [EtMIM]Cl

^{1}H-NMR spectrum of [EtMIM]Cl is shown in Figure 3 and the related parameters are listed in Table 1. Locations of hydrogen in [EtMIM]Cl are shown in Table 1 as A, B, C, D, E, and F. ^{1}H-NMR (DMSO-d_6): 1.25 ppm (t, 3H, -CH_2CH_3), 3.97 ppm (s, 3H, -NCH_3), 4.21 ppm (q, 2H), 5.47 ppm (s, 2H), 7.91 ppm (q, 2H, -NCHCHN-), and 9.56 ppm (s, 1H, -NCHN-).

Deacetylation Degree and Molecular Weight

Deacetylation degree (DD) values of chitosan (94.13 %) can be easy obtained by alkalimetry. According to equation (3), the molecular weight (M_v) of chitosan was calculated as 8.41×10^5.

Chitosan Dissolution in Ionic Liquids

The solubility data of chitosan in [BMIM]Cl and [EtMIM]Cl

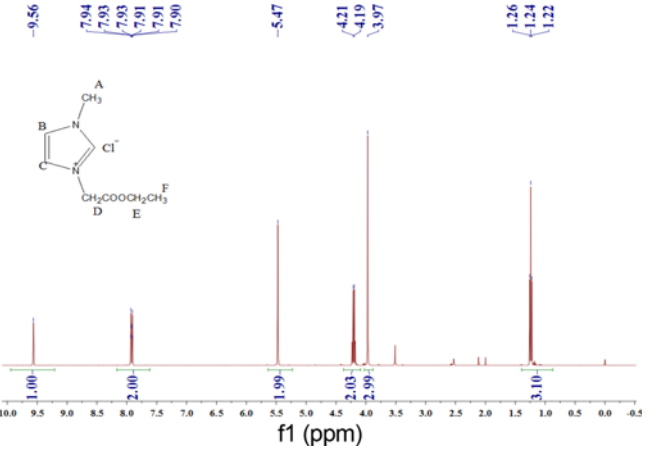

Figure 3. The ^{1}HNMR of [EtMIM]Cl.

Table 1. ^{1}HNMR Results of [EtMIM]Cl

	Chemical shift (ppm)	Split	Number of H	Location comment
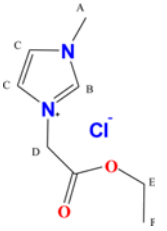	9.56	s	1	B
	7.91	q	2	C
	5.47	s	2	D
	4.21	q	2	E
	3.97	s	3	A
	1.25	t	3	F

Table 2. Solubilities of the chitosan in [BMIM]Cl and [EtMIM]Cl at different temperature

Ionic liquid	Solubility (gram per 100 g of the IL)							
	40 °C	50 °C	60 °C	70 °C	80 °C	90 °C	100 °C	110 °C
[BMIM]Cl	-	-	-	0.2	0.4	0.4	0.6	0.8
[EtMIM]Cl	-	0.4	0.6	0.8	1.4	1.8	2.4	3.2

Table 3. Solubilities and thermodynamic parameters of the chitosan in [EtMIM]Cl at different temperature

Entry	Temperature (°C)	Solubility (g/100 g IL)	Thermodynamic parameters		
			ΔG_S^θ (kJ)	ΔH_S^θ (kJ)	$T\Delta S_S^\theta$ (J)
1	40	-	-	-	-
2	50	0.4	31.004	30.422	-1.8
3	60	0.6	30.830	32.334	4.5
4	70	0.8	30.946	34.304	9.8
5	80	1.4	30.207	36.332	17.3
6	90	1.8	30.301	38.420	22.4
7	100	2.4	30.245	40.564	27.7
8	110	3.2	30.138	42.767	33.0

are listed in Table 2. It is shown that the solubility of chitosan increased with the rising of temperature. The chitosan began to dissolve in [EtMIM]Cl at 50 °C but began to dissolve in [BMIM]Cl at 70 °C. And obviously, at same dissolution temperature, the solubility of chitosan in [EtMIM]Cl were higher than that in [BMIM]Cl. Comparing the different cationic groups of [BMIM]Cl and [EtMIM]Cl, the carboxylic acid ester cationic group in $[EtMIM]^+$ has more electronegative ester groups and stronger electronic cloud density of oxygen atoms than alkyl group in $[BMIM]^+$, [EtMIM]Cl is easier to destroy the intermolecular or intramolecular hydrogen bonds in chitosan, so as to accelerate the dissolution of chitosan in [EtMIM]Cl.

The molecular simulation facts also support the different chitosan dissolution data in [BMIM]Cl and [EtMIM]Cl.

According to M_v and the solubility data of chitosan, the standard solution Gibbs energy (ΔG_S^θ) for chitosan in [EtMIM]Cl can be calculated by the following equation:

$$\Delta G_S^\theta = -RT\ln x \tag{4}$$

where T refers to temperature, R=8.314 J/(mole·K), x stands for the mole fraction of chitosan dissolved in [EtMIM]Cl. It can be seen from Figure 4 that ln x has a linear relationship with temperature.

On the basis of equation (4) and the Gibbs-Helmholtz equation, the standard solution enthalpy (ΔH_S^θ) can be calculated by the following equation [34]:

$$\Delta H_S^\theta = RT^2\left(\frac{d\ln x}{dT}\right) \tag{5}$$

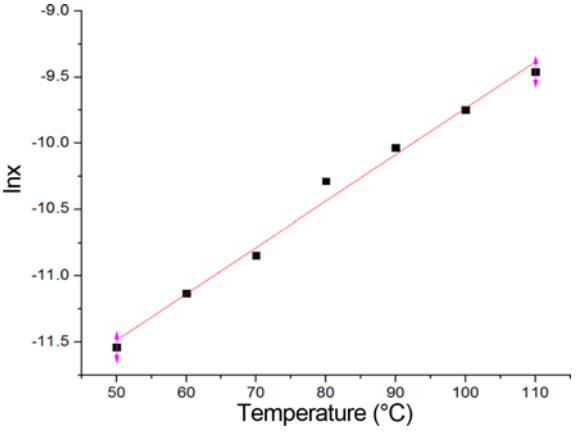

Figure 4. Plots of ln x versus temperature for chitosan in [EtMIM]Cl.

And the standard solution entropy ($T\Delta S_S^\theta$) can be calculated by the following equation:

$$T\Delta S_S^\theta = \Delta H_S^\theta - \Delta G_S^\theta \tag{6}$$

The thermodynamic parameters investigated are summarized in Table 3.

The positive ΔG_S^θ values in different temperature show that the interaction between the cation and anions might be stronger than that between chitosan and [EtMIM]Cl, and the dissolution process of chitosan was thermodynamically unfavorable. It can also be found that all the ΔH_S^θ and ΔS_S^θ values were positive when the temperature was higher than 50 °C, which means that the process of chitosan dissolved in [EtMIM]Cl was entropy-driven. And there was no driven force owing to the negative ΔS_S^θ values at 50 °C. Because these processes are all non-spontaneous, a higher temperature is necessary to increase the dissolution of chitosan in [EtMIM]Cl.

β and π^* Parameters of [EtMIM]Cl

The general dipolarity/polarizability (π^*) and the hydrogen bond basicity (β) were used to analyze the interaction between chitosan and [EtMIM]Cl, which were summarized in Table 4. β and π^* parameters were calculated by the following equation [35-38]:

$$\pi^* = 0.314(27.52 - \nu_{(DENA)}) \tag{7}$$

$$\beta = (1.035\,\nu_{(DENA)} + 2.64 - \nu_{(NA)})/2.80 \tag{8}$$

Table 4. β and π^* parameters of the [EtMIM]Cl

Parameters	$\lambda_{(DENA)}$	$\lambda_{(NA)}$	β	π^*
Values	441	447	1.337	1.520

where $\nu_{(NA)} = 1/(\lambda_{max(NA)}10^{-4})$ (9)

and $\nu_{(DENA)} = 1/(\lambda_{max(DENA)}10^{-4})$ (10)

It is known that the hydrogen bond accepting ability of anions of ILs can be measured by β values [39] and the hydrogen bond accepting ability has a positive correlation with the solubility of chitosan.

The β of [EtMIM]Cl was 1.337, higher than those β values of [AMIM]Cl and [BMIM]Cl (both 0.83) [35,36]. Comparing the different cationic groups of [EtMIM]Cl and other chloride ionic liquids, the carboxylic acid ester cationic group in $[EtMIM]^+$ has more electronegative ester groups and stronger electronic cloud density of oxygen atoms than alkyl group. [EtMIM]Cl has higher β value, which is easier to destroy the intermolecular or intramolecular hydrogen bonds in chitosan, so as to accelerate the dissolution of chitosan in [EtMIM]Cl. In other words, [EtMIM]Cl is a good solvent for chitosan.

From Table 2, the solubility of chitosan in [EtMIM]Cl were higher than that in [BMIM]Cl at same dissolution temperature.

Characterization of Chitosans

It is found that [EtMIM]Cl was soluble in methanol, and the chitosan could not be dissolved in methanol. Therefore, the chitosan dissolved in [EtMIM]Cl could be easily regenerated by adding methanol into the system. FTIR, XRD and SEM were used to study the structure of the regenerated chitosan, and the thermal characteristic was investigated by TGA.

Figure 5 shows FTIR spectra of native and regenerated chitosan from [EtMIM]Cl with different temperature. It is noted that they have similar curves. The absorption peak of the β-(1-4) stretching is at about 895 cm^{-1}, and the dissymmetry stretching vibration of the C-O-C is at about 1029 cm^{-1}. The peak at about 2914 cm^{-1} can be regarded as the -CH and $-CH_2$ stretching, and that at about 1134 cm^{-1} and 1360 cm^{-1} are the stretching absorption and O-H twisting. This shows that no chemical reactions occurred in the process of dissolution. And the peak at about 1520 cm^{-1} (variable angle vibration absorption peak of ammonium salt) was not found in the regenerated chitosan [40]. This indicates that no ammonium salt was formed and the main chain of chitosan was not completely destroyed during the dissolution process. In other words, [EtMIM]Cl was served as a kind of solvent in the process of dissolving chitosan.

Figure 6 shows TGA curves of native chitosan and regenerated chitosan. It can be found that the TGA curves were very similar at lower temperatures. Compare to the rapid decomposition temperature of native chitosan (from 270 °C to 360 °C), the regenerated chitosan had a slightly higher char yield and a lower onset temperature (under 225 °C). This result indicates that the dissolution and regeneration processes could destroy the hydrogen bonds in chitosan but could not disrupt the main chains of chitosan.

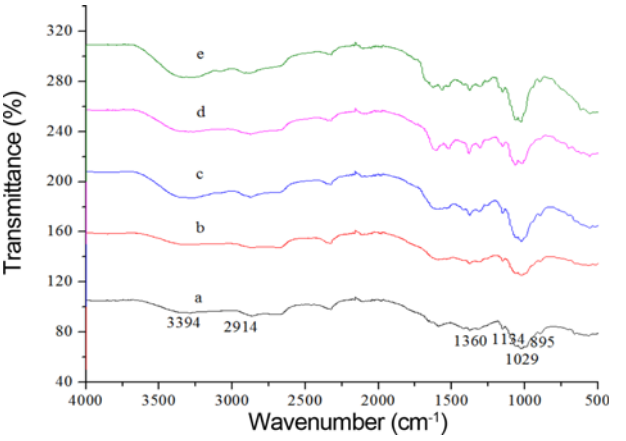

Figure 5. FTIR spectra of the native chitosan (a) and the regenerated chitosan with reaction temperature of 60 °C (b), 80 °C (c), 100 °C (d), and 120 °C (e).

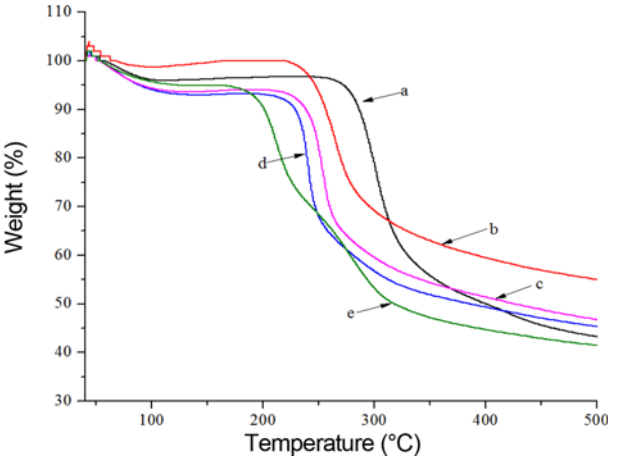

Figure 6. TGA curves of the native chitosan (a) and the regenerated chitosan with reaction temperature of 60 °C (b), 80 °C (c), 100 °C (d), and 120 °C (e).

XRD profiles of native chitosan and regenerated chitosan from the [EtMIM]Cl are shown in Figure 7. The two main diffraction peaks at 2θ=10.5 ° and 19.8 ° (shown in Figure 7(a)), assigned to (0 2 0) and (1 0 0) crystallographic planes, respectively, are typical crystalline domains of the native chitosan [41,42]. All the regenerated chitosans show diffraction peaks at about 2θ=22.6 °. The crystallization degree of the chitosan decreased sharply in the process of dissolution and regeneration, which was possibly due to the destruction of the hydrogen bonds and the native crystalline form of chitosan.

SEM surface morphology of the native chitosan and regenerated chitosan are shown in Figure 8. The regenerated chitosan membranes exhibited higher compactness than the native chitosan. And with the dissolution temperature increasing, the regenerated chitosan became more compactly. In addition, the regenerated chitosan membrane at 120 °C (Figure 8(e)) was smooth and presented a crack-free appearance.

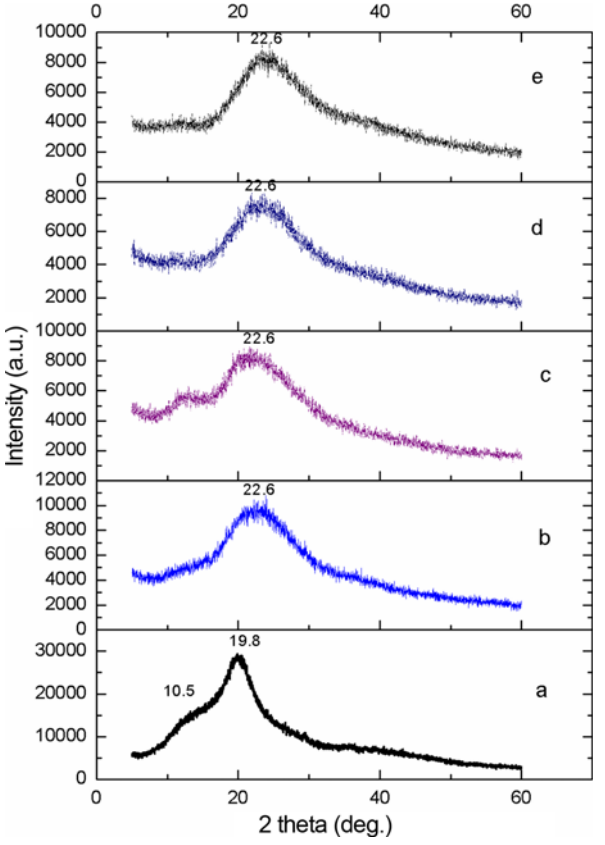

Figure 7. XRD profiles of the native chitosan (a) and the regenerated chitosan with reaction temperature of 60 °C (b), 80 °C (c), 100 °C (d), and 120 °C (e).

Dissolution Mechanism of Chitosan in [EtMIM]Cl

The electrostatic potential surfaces for chitobiose and [EtMIM]Cl are shown in Figure 9. The red regions and the blue regions represent the negative charges and the positive charges, respectively. The red regions of Cl and the ethylacetyl of $[EtMIM]^+$ can be easily attacked by protons, they may interact with the blue regions and the red regions of the chitobiose, respectively.

Figure 10 shows the optimized structure of the interaction between chitobiose and [EtMIM]Cl. The hydrogen bonds

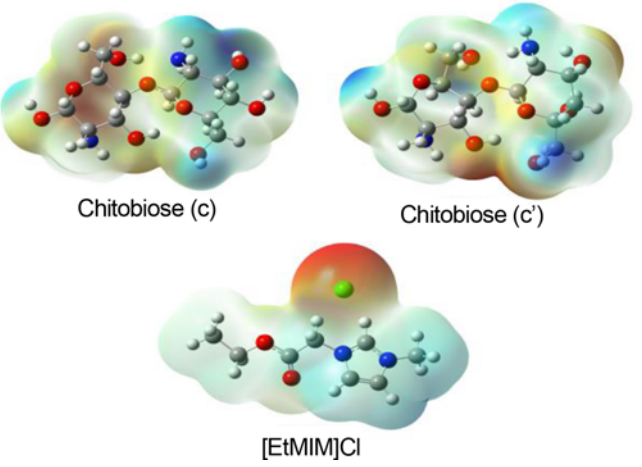

Figure 9. Electrostatic potential surfaces for chitobiose and [EtMIM]Cl optimized completely at B3LYP/6-31G(d,p) basis set.

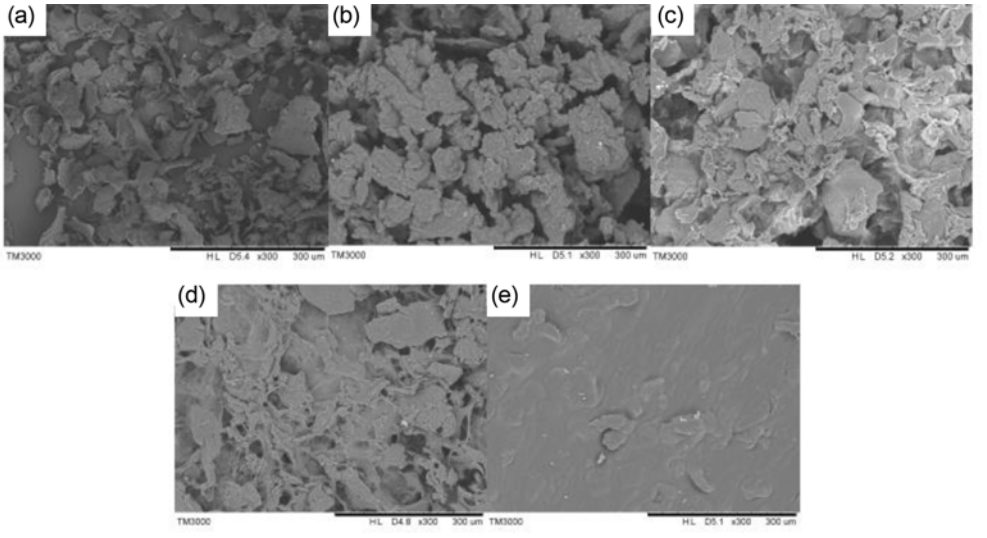

Figure 8. SEM surface morphology (magnification 300×) of the native chitosan (a) and the regenerated chitosan with reaction temperature of 60 °C (b), 80 °C (c), 100 °C (d), and 120 °C (e).

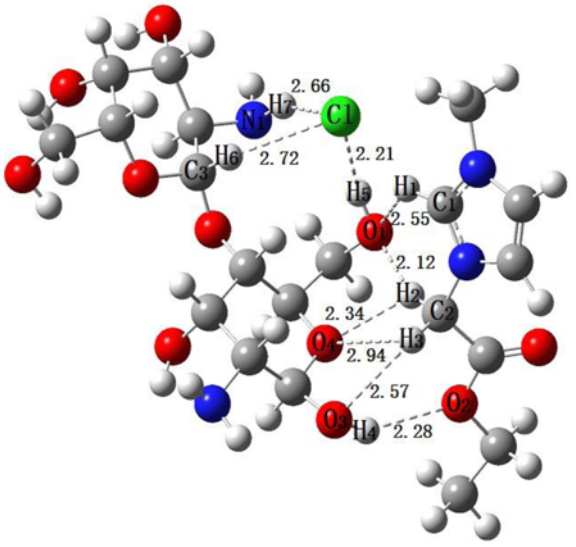

Figure 10. The optimized structure of the interaction between chitobiose and [EtMIM]Cl.

Table 5. Hydrogen bonds between [EtMIM]Cl and chitobiose

Entry	A-B bond	Bond length (Å)	Comments
1	N_1-H_7…Cl	2.66	Anion Cl^-
2	C_3-H_6…Cl	2.72	
3	O_1-H_5…Cl	2.21	
4	C_1-H_1…O_1	2.55	
5	C_2-H_2…O_1	2.12	
6	C_2-H_2…O_4	2.34	Cation $[EtMIM]^+$
7	C_2-H_3…O_4	2.94	
8	C_2-H_3…O_3	2.57	
9	O_3-H_4…O_2	2.28	

between [EtMIM]Cl and chitobiose are listed in Table 5.

As shown in Figure 10 and Table 4, five kinds of hydrogen bonds, C-H/O, O-H/O1, O-H/Cl, C-H/Cl, N-H/Cl and nine strong hydrogen bonds are found, which means the existence of strong interaction between [EtMIM]Cl and chitobiose.

The anion Cl^- of ionic liquid formed three hydrogen bonds with amino, hydroxymethyl, methylene group of pyran ring in chitobiose, including O_1-H_5…Cl (2.21 Å), N_1-H_7…Cl (2.66 Å), and C_3-H_6…Cl (2.72 Å). While the cation group $[EtMIM]^+$ of the ionic liquid formed six hydrogen bonds with the hydroxyl, hydroxymethyl, oxygen atom of pyran ring in chitobiose. The active groups in $[EtMIM]^+$, including the methylene group, C_1 atom in imidazole ring and oxygen atom of carboxylic acid ester, played important roles in hydrogen bonds formation. The oxygen atom of carboxylic ester formed strong hydrogen bond (2.28 Å) with the hydroxyl of chitobiose (O_3-H_4…O_2). Active methylene groups (C_2-H_2, C_2-H_3) of carboxylic acid ester form four hydrogen bonds with the hydroxyl, hydroxymethyl, oxygen atom of pyran ring in chitobiose. The C_1 atom of in imidazole ring formed strong hydrogen bonds (2.55 Å) with the hydroxyl of chitobiose (C_1-H_1…O_1).

The molecular simulation results indicated that both the Cl^- anions and the $[EtMIM]^+$ cation played important roles in the chitosan dissolution process, by the disruption of native hydrogen bonds of chitosan. Especially, the oxygen atom and active methylene group of carboxylic acid ester in $[EtMIM]^+$, formed strong hydrogen bonds with chitobiose.

The solubility data of chitosan in [BMIM]Cl and [EtMIM]Cl support the molecular simulation. At same dissolution temperature, the solubility of chitosan in [EtMIM]Cl were higher than that in [BMIM]Cl. The molecular simulation results indicated that both the Cl^- anions and $[EtMIM]^+$ cation played important roles in the chitosan dissolution process.

Conclusion

In this paper, an ionic liquid, [EtMIM]Cl, was synthesized to explore the dissolution and regeneration behavior of chitosan. The possible interactions between chitosan and [EtMIM]Cl have been investigated. It can be seen that [EtMIM]Cl cannot dissolve chitosan when the temperature was below 50 °C and the solubility of chitosan increased with the rise of temperature. All processes were non-spontaneous and it was necessary to use a higher temperature to increase the dissolution of chitosan in [EtMIM]Cl.

The main chain of chitosan had not been destroyed during the dissolution of chitosan in [EtMIM]Cl. In addition, the hydrogen bonds of native chitosan might be destroyed in the process of dissolution and new hydrogen bonds could be formed between chitosan and [EtMIM]Cl.

Density functional theory (DFT) computations were performed to study the interactions between the [EtMIM]Cl and chitobiose. Five kinds of hydrogen bonds, C-H/O, O-H/O1, O-H/Cl, C-H/Cl, N-H/Cl were found, which means the existence of strong interaction between [EtMIM]Cl and chitobiose. Especially, the oxygen atom and active methylene group of carboxylic acid ester in $[EtMIM]^+$, formed strong hydrogen bonds with chitobiose. The molecular simulation results indicated that both the Cl^- anions and the $[EtMIM]^+$ cation played important roles in the chitosan dissolution process, by the disruption of native hydrogen bonds of chitosan. The information obtained here would provide a guide for the design and syntheses of novel solvent systems for the dissolution of chitosan.

Acknowledgements

This work was supported by Natural Science Foundation of Jiangsu Province (No. BK2011799, BK20140939), National Natural Science Foundation of China (No. 21203094,

21373112) and the specialized research fund for the Doctoral Program of Higher Education of China (No. 20113221120006). The authors also gratefully appreciate the support from Jiangsu Overseas Research & Training Program for University Prominent Young & Middle-aged Teachers and Presidents.

References

1. A. M. Dias, A. R. Cortez, M. Barsan, J. Santos, and C. M. Brett, *ACS Sustain. Chem. Eng.*, **1**, 1480 (2013).
2. F. B. Lv, C. X. Wang, P. Zhu, and C. J. Zhang, *Cellulose*, **21**, 4405 (2014).
3. W. Jiang, Z. M. Zhou, D. Wang, X. H. Zhou, R. Y. Tao, Y. Yang, Y. X. Shi, G. L. Zhang, D. Y. Wang, and Z. Zhou, *Carbohydr. Polym.,* **153**, 105 (2016).
4. M. Dash, F. Chiellini, R. Ottenbrite, and E. Chiellini, *Prog. Polym. Sci.*, **36**, 981 (2011).
5. X. F. Sun, Q. Q. Tian, and Z. M. Xue, *RSC Adv.*, **4**, 30282 (2014).
6. A. Ayoub, R. A. Venditti, J. J. Pawlak, A. Salam, and M. A. Hubbe, *ACS Sustain. Chem. Eng.*, **1**, 1102 (2013).
7. L. Qian and H. F. Zhang, *Green Chem.*, **12**, 1207 (2010).
8. R. Hirase, Y. Higashiyama, M. Mori, Y. Takahara, and C. Yamane, *Carbohydr. Polym.*, **80**, 993 (2010).
9. Z. Zhang, A. A. M. Salih, M. T. Li, and B. L. Yang, *Energ. Fuel.,* **28**, 2802 (2014).
10. E. B. Silva, D. Santos, D. R. M. Alves, M. S. Barbosa, R. C. L.Guimaraes, B. M. S. Ferreira, R. A. Guarnieri, E. Franceschi, C. Dariva, and A. F. Santos, *Energ. Fuel.,* **27**, 6311 (2013).
11. Z. W. Wu, C. Chen, Q. Guo, B. X. Li, Y. G. Que, L. Wang, H. Wan, and G. F. Guan, *Fuel*, **184**, 128 (2016).
12. J. P. Hallett and T. Welton, *Chem. Rev.*, **111**, 3508 (2011).
13. I. Anugwom, V. Eta, P. Virtanen, P. M. Arvela, M Hedenstrcm, M. Hummel, H. Sixta, and J. P. Mikkola, *ChemSusChem*, **7**, 1170 (2014).
14. A. M. da Costa Lopes and R. Bogel-Łukasik, *ChemSusChem*, **8**, 947 (2015).
15. M. E. Zakrzewska, E. Bogel-Lukasik, and R. Bogel-Lukasik, *Energ. Fuel.,* **24**, 737 (2010).
16. F. Niroomand, A. Khosravani, and H. Younesi, *Cellulose*, **23**, 1311 (2016).
17. Z. H. Liu, X. F. Sun, M. Y. Hao, C. Y. Huang, Z. M. Xue, and T. C. Mu, *Carbohydr. Polym.*, **117**, 99 (2015).
18. J. J. Miao, Y. Q. Yu, Z. M. Jiang, and L. P. Zhang, *Cellulose*, **23**, 1209 (2016).
19. N. Sun, H. Rordriguez, M. Rahman, and R. D. Rogers, *Chem. Commun.*, **47**, 1405 (2011).
20. B. Zhao, L. Greiner, and W. Leitner, *RSC Adv.*, **2**, 2476 (2012).
21. V. Vladimira and K. Katerina, *RSC Adv.*, **5**, 17690 (2015).
22. Z. Q. Pang, C. H. Dong, and X. J. Pan, *Cellulose*, **23**, 323 (2016).
23. X. Y. Liu, P. R. Chang, P. W. Zheng, D. P. Anderson, and X. F. Ma, *Cellulose*, **22**, 709 (2015).
24. W. J. Xiao, Q. Chen, Y. Wu, T. Wu, and L. Dai, *Carbohydr. Polym.*, **83**, 233 (2011).
25. X. F. Sun, Z. M. Xue, and T. Mu, *Green Chem.*, **16**, 2102 (2014).
26. J. M. Zhang, H. Zhang, J. Wu, J. Zhang, J. S. He, and J. F. Xiang, *Phys. Chem. Chem. Phys.*, **12**, 1941 (2010).
27. Y. Zhao, X. Liu, J. Wan, and S. Zhang, *Phys. Chem. Phys. Chem*, **13**, 3126 (2012).
28. N. Gathergood, M. T. Garcia, and P. J. Scammells, *Green Chem.*, **6**, 166 (2004).
29. R. Lungwitz and S. Spange, *New J. Chem.*, **32**, 392 (2008).
30. Y. Fukaya, A. Sugimoto, and H. Ohno, *Biomacromolecules*, **7**, 3295 (2006).
31. C. Loerbroks, R. Rinaldi, and W. Thiel, *Chem. Eur. J.*, **19**, 16282 (2013).
32. Q. Q. Tian, S. Y. Liu, X. F. Sun, H. T. Sun, Z. M. Xue, and T. C. Mu, *Carbohydr. Res*., **408**, 107 (2015).
33. M. J. Frisch, G. W. Trucks, H. B. Schlegel, G. E. Scuseria, M. A. Robb, J. R. Cheeseman, G. Scalmani, V. Barone, B. Mennucci, G. A. Petersson, H. Nakatsuji, M. Caricato, X. Li, H. P. Hratchian, A. F. Izmaylov, J. Bloino, G. Zheng, J. L. Sonnenberg, M. Hada, M. Ehara, K. Toyota, R. Fukuda, J. Hasegawa, M. Ishida, T. Nakajima, Y. Honda, O. Kitao, H. Nakai, T. Vreven, J. A. Montgomery, Jr., J. E. Peralta, F. Ogliaro, M. Bearpark, J. J. Heyd, E. Brothers, K. N. Kudin, V. N. Staroverov, R. Kobayashi, J. Normand, K. Raghavachari, A. Rendell, J. C. Burant, S. S. Iyengar, J. Tomasi, M. Cossi, N. Rega, J. M. Millam, M. Klene, J. E. Knox, J. B. Cross, V. Bakken, C. Adamo, J. Jaramillo, R. Gomperts, R. E. Stratmann, O. Yazyev, A. J. Austin, R. Cammi, C. Pomelli, J. W. Ochterski, R. L. Martin, K. Morokuma, V. G. Zakrzewski, G. A. Voth, P. Salvador, J. J. Dannenberg, S. Dapprich, A. D. Daniels, Ö. Farkas, J. B. Foresman, J. V. Ortiz, J. Cioslowski, and D. J. Fox, Gaussian 09, Revision B.01, Gaussian, Inc., Wallingford CT, 2009.
34. A. J. Queimada, F. L. Mota, S. P. Pinho, and E. A. Macedo, *J. Phys. Chem. B*, **113**, 3469 (2009).
35. Y. Fukaya, A. Sugimoto, and H. Ohno, *Biomacromolecules*, **7**, 3295 (2006).
36. L. K. J. Hauru, M. Hummel, A. W. T. King, I. Kilpelainen, and H. Sixta, *Biomacromolecules*, **13**, 2896 (2012).
37. C. Reichardt, *Green Chem.*, **7**, 339 (2005).
38. S. K. Shukla, N. D. Khupse, and A. Kumar, *Phys. Chem. Chem. Phys.*, **14**, 2754 (2012).
39. C. Chiappe and D. Pieraccini, *J. Phys. Org. Chem.*, **18**, 275 (2005).
40. Q. T. Chen, A. R. Xu, Z. Y. Li, J. J. Wang, and S. J. Zhang, *Green Chem.*, **13**, 3446 (2011).
41. C. Stefanescu, W. H. Daly, and I. I. Negulescu, *Carbohydr. Polym.*, **87**, 435 (2012).
42. B. M. Ma, X. L. Hou, and C. J. He, *Fiber. Polym.*, **16**, 2704 (2015).